Published in final edited form as:
Toxicol Sci. 2019 February 01; 167(2): 347–359. doi:10.1093/toxsci/kfy236.

The Impact of Scaling Factor Variability on Risk-Relevant Pharmacokinetic Outcomes in Children: A Case Study Using Bromodichloromethane (BDCM)

Elaina M. Kenyon[*,1], **John C. Lipscomb**[†], **Rex A. Pegram**[*], **Barbara J. George**[*], **Ronald N. Hines**[*]

[*]U.S. EPA, ORD/NHEERL, RTP, North Carolina

[†]U.S. EPA, ORD/NHSRC, Cincinnati, Ohio

Abstract

Biotransformation rates extrapolated from *in vitro* data are used increasingly in human physiologically based pharmacokinetic (PBPK) models. This practice requires use of scaling factors, including microsomal content (mg of microsomal protein/g liver, MPPGL), enzyme specific content, and liver mass as a fraction of body weight (FVL). Previous analyses indicated that scaling factor variability impacts pharmacokinetic (PK) outcomes used in adult population dose-response studies. This analysis was extended to pediatric populations because large inter-individual differences in enzyme ontogeny likely would further contribute to scaling factor variability. An adult bromodichloromethane (BDCM) model (Kenyon, E. M., Eklund, C., Leavens, T. L., and Pegram, R. A. (2016a). Development and application of a human PBPK model for bromodichloromethane (BDCM) to investigate impacts of multi-route exposure. *J. Appl. Toxicol.* 36, 1095–1111) was re-parameterized for neonates, infants, and toddlers. Monte Carlo analysis was used to assess the impact of pediatric scaling factor variation on model-derived PK outcomes compared with adult findings. BDCM dose metrics were estimated following a single 0.05-liter drink of water or a 20-min bath, under typical (5 μg/l) and plausible higher (20 μg/l) BDCM concentrations. MPPGL, CYP2E1, and FVL values reflected the distribution of reported pediatric population values. The impact of scaling factor variability on PK outcome variation was different for each exposure scenario, but similar for each BDCM water concentration. The higher CYP2E1 expression variability during early childhood was reflected in greater variability in predicted PK outcomes in younger age groups, particularly for the oral exposure route. Sensitivity analysis confirmed the most influential parameter for this variability was CYP2E1, particularly in neonates. These findings demonstrate the importance of age-dependent scaling factor variation used for *in vitro* to *in vivo* extrapolation of biotransformation rates.

Keywords

in vitro to *in vivo* extrapolation (IVIVE); scaling factors; variation; age groups; pediatric

[1]To whom correspondence should be addressed at U.S. EPA, 109 TW Alexander Dr, Maildrop B105-03, Research Triangle Park NC 27711, Fax (919) 541-4284; kenyon.elaina@epa.gov.

SUPPLEMENTARY DATA
Supplementary data are available at *Toxicological Sciences* online.

For pediatric populations, physiologically based pharmacokinetic (PBPK) models provide a powerful computational framework to integrate knowledge related to growth-related changes in physiology with age-dependent changes in molecular parameters related to xenobiotic biotransformation, protein binding, and transporter function (Prasad et al., 2016; Sethi et al., 2016; Yoon and Clewell, 2016). PBPK models provide a means to evaluate age-dependent changes in pharmacokinetics (eg, measures of internal dose) as one factor contributing to the potential for age-dependent sensitivity to chemical exposures, particularly when combined with age-appropriate exposure scenarios (Yoon and Clewell, 2016).

Biotransformation rate parameters (Vmax, Km) determined *in vitro* using human hepatic subcellular fractions (microsomes, cytosol) or hepatocytes are increasingly available for use in human PBPK models. Use of human biotransformation rate parameters eliminates the uncertainty associated with biotransformation rate parameter interspecies extrapolation, but adds a new source of uncertainty in that *in vitro* to *in vivo* extrapolation (IVIVE) is necessary. IVIVE for Vmax is accomplished computationally within a PBPK model using scaling factors such as mg microsomal protein (MSP) per gram of liver (MPPGL) or the number of hepatocytes per gram of liver depending on the experimental system used, as well as liver mass as a fraction of body weight (FVL). Also, in some cases, expression levels of a specific enzyme are incorporated if the enzyme primarily responsible for a specific biotransformation step is known (Lipscomb and Poet, 2008).

Historically, most PBPK models treat parameters (physiological and molecular) as constants or point estimates, although in reality, they are associated with marked interindividual variability within the human population. This intrinsic variability is particularly notable for pediatric biotransformation rate parameters needed for IVIVE. Specifically, changes in xenobiotic metabolizing enzyme (XME) expression are substantial during both the fetal period and first one to two years after birth and are highly dependent on the particular XME (Hines, 2008, 2012). For example, in the case of CYP2E1, which metabolizes many low molecular weight organic chemicals, 80-fold variation was seen in hepatic expression levels during the neonatal period (0–30 days) in a large study that encompassed both pre-natal and postnatal periods (Johnsrud et al., 2003). In this same study, expression was low in the neonatal age group (0–70 pmol/mg MSP; median = 8.8 pmol/mg MSP) and less than older infants (31–90 days, 10–43 pmol/mg MSP; median = 23.8 pmol/mg MSP) or children (91 days–18 years, 18–95 pmol/mg MSP; median = 41.4 pmol/mg MSP).

High variability and altered XME expression levels do not necessarily result in altered pharmacokinetics. For example, Kedderis (1997) found that although enzyme induction has the effect of increasing the rate and extent of biotransformation *in vitro*, this may not be quantitatively reflected *in vivo* due to physiological limitations such as blood flow to liver. Specifically, at typical low environmental exposure levels, highly variable enzyme expression or level of activity may not affect clearance if the rate-limiting step in metabolic biotransformation is rate of chemical delivery in blood to the liver rather than biotransformation of the parent chemical. Given the high level of XME expression variability and reduced XME expression in the neonatal and/or infant period for some

enzymes, there is a strong case for using a PBPK framework to evaluate the effect of such differences in the context of realistic physiological and exposure scenarios.

Bromodichloromethane (BDCM) is a drinking water disinfection byproduct (DBP) and is the second most prevalent of the trihalomethane class of DBPs. At low exposure levels, BDCM is predominantly metabolized in humans by CYP2E1 (Zhao and Allis, 2002). BDCM was selected for this case study because its volatility and skin permeability make multi-route exposure a concern; multiple pharmacokinetic (PK) outcomes also are of interest as measures of internal dose or biomarkers of exposure (Kenyon et al., 2016a; USEPA, 2005). In addition, based on water use patterns (Lynberg et al., 2001; Nuckols et al., 2005), BDCM exposure is a concern across all age groups.

In our previous work (Kenyon et al., 2016b), we found that variability in the IVIVE biotransformation rate scaling factors can have important route-dependent impacts on PK outcomes under environmentally relevant exposure scenarios in adults. Because of the known large variability in the ontogeny of various XMEs during fetal development and early childhood, including CYP2E1 (Hines, 2008; Johnsrud et al., 2003), we have extended this earlier work to evaluate the extent to which variability in CYP2E1 hepatic protein expression, relative liver mass and MPPGL during early childhood is reflected in predicted PK outcomes. Monte Carlo analysis was used with BDCM as a model chemical under environmentally relevant exposure scenarios (Thomas et al., 1996; USEPA, 1997).

MATERIALS AND METHODS

A published adult human PBPK model for BDCM (Kenyon et al., 2016a) was re-parameterized for three pediatric age groups: 0–30 days (neonate), 31–90 days (infant), and 91 days–2 years of age (toddler). These intervals were selected based on the age groups identified in Johnsrud et al. (2003) that correspond to the CYP2E1 developmental trajectory that minimizes differences within while maximizing differences between age groups. The pediatric CYP2E1 hepatic protein expression data are described in greater detail in the Supplementary material and are part of a larger published database for XME ontogeny (McCarver et al., 2017).

The model structure (see Supplementary Figure 1) and assumptions have been described in detail elsewhere; this model adequately predicted BDCM blood concentrations in studies of adult volunteers during water use exposures involving drinking, bathing and showering (Kenyon et al., 2016a). Model structure, assumptions, and chemical-specific parameters for this analysis are the same as those used previously (Kenyon et al., 2016a,b). Adult physiological parameters are provided in Table 1, and many are the same as those used previously with some specific exceptions. Alveolar ventilation rate (QPC), alveolar deadspace, ratio of QPC to cardiac output and fat volume were updated to use the more comprehensive sources used for pediatric parameters (Brochu et al., 2006, 2011, 2012; Brown et al., 1997; Haddad et al., 2001). Organ volumes (Table 1) for pediatric age groups were calculated on the basis of the equations presented in Haddad et al. (2001) with total body fat calculated on the basis of Price et al. (2003). Blood flows for pediatric populations were primarily derived from Edginton et al. (2006) and other physiological parameters were

obtained from the literature as detailed in footnotes to Table 1 (Brochu et al., 2006, 2011, 2012; Laurent et al., 2007; Saitoh et al., 2015).

Chemical-specific parameters are provided in Table 2. Partition coefficients were treated as invariant across age groups. Available data indicate that blood: air partition coefficients for volatile organic compounds do not differ between adult and pediatric populations (Mahle et al., 2007). In addition, tissue lipid and water composition does not differ substantively as a function of age from newborn to young adult for healthy tissues (White et al., 1991). Other chemical-specific parameters were the same as used in our previous analysis (Kenyon et al., 2016b) and treated as invariant across age groups. The Vmax for hepatic CYP2E1-mediated BDCM metabolism (VmaxBDCM) in units of μg/h-kg was made specific for each age group and calculated within the model code during each simulation using the equation:

$$\mathrm{VmaxBDCM} = \textit{in vitro}\ \mathrm{Vmax} \times \mathrm{MPPGL} \times \mathrm{CYP2E1} \times \mathrm{FVL}, \quad (1)$$

where the *in vitro* Vmax is in units of μg/h-pmol CYP2E1 (Table 2), MPPGL is in units of mg MSP/g liver, CYP2E1 is in units of pmol CYP2E1 protein/mg MSP and FVL is in units of g liver/kg BW (Table 3). Distributional characteristics are provided in Table 3 and were based on data from Johnsrud et al. (2003), McCarver et al. (2017), Lipscomb et al. (1997, 2003a,b), and Young et al. (2009). These data sets were selected because the complete original data were available enabling calculation of all needed distributional descriptors (Table 3) and descriptive statistics (Supplementary Table 1). Because subject age was available in these data sets, but measured data for MPPGL were not collected, MPPGL was estimated for each subject using the age-based equation published by Barter et al. (2008). FVL, MPPGL, and CYP2E1 were assumed to vary independently (Lipscomb et al., 2003a,b).

Distributions for FVL and MPPGL, normal and lognormal, respectively, were selected consistent with USEPA (2011b). Lower and upper bounds for FVL and MPPGL were set at the minimum and maximum values from the original data sets. Distributions for CYP2E1 were fitted using the SAS SEVERITY procedure (SAS Institute Inc, 2013) because 8 of the 42 neonatal CYP2E1 protein expression measurements were below the limit of detection. The SAS SEVERITY procedure is appropriate when there are below-detection, left-censored data and uses maximum likelihood to estimate distribution parameters. Lognormal and gamma distributions were considered for each of the age groups using the Akaike information criterion (AIC), corrected AIC (AICC), and Bayesian information criterion (BIC) as the selection criteria. For consistency, the gamma distribution was selected for all age groups because it was either a better fit (neonates) or virtually indistinguishable from the lognormal distribution (Supplementary Table 2). Input parameter distributions and values are given in Table 3.

Monte Carlo analysis was used to assess effects of variability in model input parameters, CYP2E1, MPPGL, and FVL, on PK outcomes (Figure 1). The Monte Carlo method was used to randomly sample CYP2E1, MPPGL, and FVL from defined distributions (Table 3) to estimate Vmax for BDCM within the model. Running the model for 10 000 iterations provided PK outcome data for which summary descriptive statistics were calculated. Two

exposure scenarios (single 0.05-liter drink or 20-min bath) were simulated to encompass the range of relevant exposure routes for BDCM (Kenyon et al., 2016b) at typical (5 μg/l) and plausibly high (20 μg/l) water concentrations across age groups; total simulation length was 2 h for all scenarios. PK model outcomes evaluated were area under the curve (AUC) for BDCM in venous blood (AUCv), amount of BDCM metabolized in liver (AML), maximum BDCM concentration in blood (CVmax), and maximum concentration of BDCM in exhaled breath (CalvMax). Model responses selected for evaluation were those that were either likely to be measured in water use studies (blood concentration, exhaled breath) as well as pharmacokinetically-relevant measures of internal dose (AUCv, AML). The workflows for the methods used in this analysis are illustrated in Figure 1.

Global sensitivity analysis (GSA) was performed in AcslXtreme 3.0.2.1 using the Morris method (Morris, 1991) to provide a relative ranking of importance for all model parameters. To implement the Morris GSA method in AcslXtreme, it is necessary to set ranges for input parameters that are allowed to vary under the assumption of a uniform distribution, which is considered appropriate for a screening level analysis. For physiological parameters, partition coefficients and the dermal absorption coefficient, ranges were set as ± one standard deviation from the average value used in the model (Tables 1 and 2) assuming a coefficient of variation of 30%. This assumption has been used in reverse dosimetry applications of PBPK models (Tan et al., 2007). Variation in VmaxBDCM was set based on available data (Table 3) and the range of variation for all other chemical-specific parameters was as described in Kenyon et al. (2016b). Algorithmic settings used in the analysis were 100, 25, and 1000, for p, jump, and Ns, respectively. p is the number of values in discretized parameter range (divides parameter range into p-1 ranges or hypercubes); jump is the step size in computing effects (effectively computing a number of local sensitivities); Ns is the number of samples (AEgis Technologies, 2010). These algorithmic settings were selected to optimize analysis performance; ie, multiple test runs were done until no changes were seen in the overall ranking.

RESULTS

Pharmacokinetic outcome results from the Monte Carlo simulations for oral exposure at 5 μg/l across age groups are shown in Figures 2A and 2B and Table 4 for AUCv, AML, and CVmax, respectively. Corresponding figures and tables for the 20 μg/l oral exposure are in Supplementary material (Supplementary Figs 2A and 2B, Table 3). For all PK outcomes, variability was greater in the neonate compared with other pediatric age groups or adults as assessed by coefficient of variation (%CV) and ratio of 95th to 5th percentile. For AUCv, CVmax and CalvMax, concentrations were higher in pediatric age groups compared with adults due to the smaller body mass in the former (eg, 3.81 kg neonate vs 80.8 kg adult, Table 1), ie, the same absolute amount is distributed into a smaller volume. For CalvMax, the % CV and ratio of 95th to 5th percentile values are the same as CVmax, and the concentrations are uniformly approx. 17-fold lower across age groups for CalvMax (model results not shown) compared with CVmax. The total amount of BDCM metabolized in liver (Figure 2B) was similar across age groups because metabolism is not saturated under this oral exposure scenario and overall liver metabolic capacity is not exceeded (Kenyon et al., 2016a). Results were essentially the same for the 20 μg/l exposure scenarios; the observed

dose-dependent differences in the parameters were approx. 4-fold because the processes of absorption, disposition, metabolism and excretion are within the linear range at this exposure level.

Results from the Monte Carlo simulations for bathing exposure at 5 μg/l across age groups are shown in Figures 3A and 3B and Table 5 for AUCv, AML, and CVmax, respectively. Corresponding figures and tables for the 20 μg/l bathing exposure are in Supplementary material (Supplementary Figs 3A and 3B, Table 4). As with the oral exposure, all PK outcomes for bathing exposure displayed greater variability in the neonate compared with other pediatric age groups and adults based on %CV and ratio of 95th to 5th percentile values. However, compared with oral exposure, the extent of variability was not as large between PK outcomes. Concentrations for AUCv, and CVmax were generally greater for younger age groups although cross-age group differences were not substantial. For CalvMax, the % CV and ratio of 95th to 5th percentile values are the same as CVmax, and the concentrations are uniformly approx. 17-fold lower across age groups for CalvMax (model results not shown) compared with CVmax. The total amount of BDCM metabolized in liver was greater in adults compared with pediatric age groups (Figure 3B) due to relatively greater uptake of parent chemical and delivery to the liver via combined dermal and inhalation exposure for adults during bathing.

Quantitative results for GSA using the Morris screening method are illustrated graphically in Figure 4 (AUCv) and Figure 5 (AML) for oral and Figure 6 (AUCv) and Figure 7 (AML) for bathing exposure to 5 μg/l BDCM in water; the A and B panels in these figures reflect neonates and adults, respectively, because these two age groups show the largest and smallest variation in PK outcomes, respectively. In these figures, the mean sensitivity coefficient for each parameter (averaged over the time period of the simulation) is plotted on the x-axis (μ) and the corresponding standard deviation (σ) is plotted on the y-axis to display the overall screening level GSA results. This presentation format provides an overall quantitative sense of how parameters compare with each other in terms of their relative influence on the PK outcome of interest (McNally et al., 2011). Further detail is presented in corresponding Supplementary Tables 5–8 in the Supplementary material. For oral exposure in both neonates and adults, the parameters that were most influential for AUCv were those governing absorption (KABDCM), relative liver mass (FVL), and biotransformation via the CYP2E1 pathway (CYP2E1, KM1BDCM). These same parameters also were influential for the amount of BDCM metabolized in liver (AML). CYP2E1 was the most influential parameter for AUCv and AML for both adults and neonates, although by comparison this was more strongly evident in neonates for AML. For the bathing exposure scenario, a number of parameters were highly influential for both AUCv and AML in neonates and adults; the parameters identified as influential in adults were similar to previous sensitivity analysis for this model (Kenyon et al., 2016a). What is evident for both neonatal AUCv and AML PK outcomes compared with adults is the relatively higher ranking of CYP2E1 in neonates. MPPGL was generally in the middle third of relative rankings among parameters for all PK outcomes in both adults and neonates.

DISCUSSION

Our results clearly demonstrate that variability in the development of hepatic XMEs in early childhood contributes to greater variability in predicted pharmacokinetic outcomes for early life stages compared with adults. The PBPK modeling framework is a particularly strong approach for this purpose because it incorporates relevant environmental exposures and known pediatric-specific physiological and molecular parameters using a validated model that estimates both internal dose measures and biomarkers of exposure. Use of this framework allowed for the integration of diverse information to provide a physiologically and environmentally realistic context in which to evaluate the impact of observed interindividual differences in XME ontogeny. This framework also can account for other physiological factors that may differ across life stages (Yoon and Clewell, 2016) including plasma binding protein expression (Sethi et al., 2016) and hepatic drug transporters (Prasad et al., 2016; Thomson et al., 2016).

In this case study, PK outcomes exhibited greater variability (as assessed by %CV and ratio of 95th to 5th percentile values) at younger postnatal ages for both oral and bathing exposure, although variability was generally less pronounced for the bathing exposure scenario. For the oral exposure scenario, variation in hepatic scaling factors for pediatric age groups had the greatest impact on pharmacokinetic outcomes (AUCv, CVmax, CalvMax) compared with adults. There was also greater variability in neonates compared with adults for hepatic biotransformation (AML), although it was relatively less compared with other pharmacokinetic outcomes. The overall findings in adults were similar to our earlier work in adults (Kenyon et al., 2016b). The most likely explanation for the relatively lower variation across age groups in AML compared with other PK outcomes is that at typically low environmental exposure concentrations, hepatic biotransformation is not saturated (Kenyon et al., 2016a); delivery of parent chemical to liver in blood is the rate limiting step in hepatic biotransformation under these exposure conditions. For bathing exposures, there was relatively greater variability in neonates compared with adults, although the magnitude of variation (% CV, ratio of 95th to 5th percentiles) was relatively less compared with oral exposures. Lesser impact for bathing compared with oral exposures is partially attributable to the physiology of inhalation and dermal absorption; compounds absorbed into the systemic circulation are not immediately subject to first-pass metabolism in liver or intestine, as are compounds delivered orally (Lehman-McKeeman, 2013).

Global sensitivity analysis for all model parameters using a screening method such as Morris (1991) provides a relative sense of specific parameter influence for a given exposure scenario and PK outcome for individual age groups; another advantage of GSA in general is that it allows incorporation of observed parameter variability (McNally et al., 2011). In this analysis, we looked at neonatal and adult groups because these groups demonstrated the largest and smallest predicted variability in PK outcomes, respectively, based on the Monte Carlo analysis. For neonates, CYP2E1 specific content was consistently either the most influential parameter or in the top 10% of influential parameters for all PK outcomes for both oral and bathing exposure scenarios. In adults, this was also true for oral, but not bathing exposure. Relative liver mass (FVL) was generally in the top 1/3 of influential parameters for neonates in all cases, but for adults, only for oral, not bathing exposure.

A novel aspect of our model is use of the gamma distribution without lower and upper bounds to parameterize CYP2E1. Most PBPK models assume a lognormal distribution for XME content or biochemical parameters such as Vmax (Lipscomb et al., 2003a,b; Tan et al., 2007; USEPA, 2011b). Use of the gamma distribution in our analysis for CYP2E1 parameterization has both statistical, and biological rationale. Based on AIC, AICC, and BIC information criteria, gamma distributions gave better fits for the neonate and infant CYP2E1 data than lognormal distributions and the lognormal distribution was not compellingly superior to the gamma distribution for other age groups (Supplementary Table 2). The gamma CYP2E1 parameterization without truncation for neonates has an important biological basis in that it supports representation of no functional protein present, the mode for neonate CYP2E1 in the Johnsrud et al. (2003) data. An empirical assessment of the effect of the seed used to randomly sample CYP2E1 for model input to the Monte Carlo analysis for neonate oral exposure demonstrated that the ratio of 95th to 5th percentiles was relatively stable in contrast to the ratio of the max to the min (Supplementary Table 9).

In general, MPPGL ranked in the middle third or lower among influential parameters for both neonates and adults. The relatively lesser influence of MPPGL in our model, in part, corresponds to the dependence of its input distribution on values predicted by the 2008 Barter regression equation, which is a function of age. One limitation of the Barter equation is that it accounted for only 10% of the variability in observed data used in its development (Barter et al., 2008). Using this equation results in less variability in MPPGL in younger age groups which also contributes to making this parameter relatively lower in influence on PK outcomes in general, particularly in neonates. Reassuringly, recently published measurements of MPPGL in neonates as determined using the total cytochrome P450 method (De Bock et al., 2014) fall within the range of values predicted by the equation of Barter et al. (2008).

Another source of uncertainty in model outputs is the assumption that FVL, MPPGL and CYP2E1 are independent. If this assumption is inaccurate, the model outputs may reflect excess variability (Thomas et al., 1996). Chemical-specific model parameters were treated as invariant across age groups and there is data to support this assumption for partition coefficients (Mahle et al., 2007; White et al., 1991). However, in the case of the skin diffusion coefficient (KABDCM), evidence suggests that the skin of the neonate is more fragile and permeable to pharmaceuticals compared with adult skin (Blume-Peytavi et al., 2016). This could result in increased absorption of BDCM into the systemic circulation following dermal exposure in pediatric populations.

This work was possible because of the existence of a large data base on pediatric XME expression in liver spanning both pre-natal and early childhood life stages for a large array of enzymes (McCarver et al., 2017). The unique value of such a database is that the information can be utilized to predict biotransformation and its associated variability for pediatric age groups for any chemical provided the XMEs responsible for its biotransformation and an *in vitro* rate of biotransformation for the specific chemical are known. Further classifying XMEs according to expression trajectories during pre- and post-natal development can facilitate identification of chemicals that are a higher priority

for evaluation when considered together with information on exposure potential in pediatric populations.

Another PBPK-based risk analysis application for XME ontogeny data was demonstrated by Nong et al. (2006). These authors assessed the impact of variability in both physiological parameters and CYP2E1 expression on AUC for toluene in blood using a scenario of 1 ppm toluene exposure for 24 h. Using the 5th, 50th, and 95th percentiles for predicted AUC, Nong et al. (2006) calculated intragroup and adult-child factors; the intragroup variability factor was calculated as the ratio of the 95th percentile value over the 50th percentile value for the same age group, and the adult-child variability factor was calculated as the ratio of the 95th percentile value for the child over the 50th percentile value for the adult. Intragroup factors varied between 1.07 and 1.48 and adult-child variability factors ranged from 3.88 to 1.35 from neonate to adolescent. The intragroup variability factor provides an another way to compare variability between age groups, much as the %CV and ratio of 95th to 5th percentile used in Tables 4 and 5, and Figures 2 and 3, Supplementary Figures 2 and 3 in this study. The calculated adult-child variability factor is specific for this chemical exposure scenario (inhalation) and dose metric (AUC). The adult-child variability factor is analogous to the PK portion of the default uncertainty factor for interindividual variability ($UF_HTK = 3$) and has also been used in risk analysis as a chemical-specific adjustment factor (CASF; IPCS, 2005) or data-derived extrapolation factor (DDEF; USEPA, 2014) to avoid the application of default uncertainty factors.

We performed a similar analysis to that of Nong et al. (2006) for AUCv (Table 6) and AML (Table 7) based on both oral and bathing exposures for BDCM (1) to compare general intragroup trends across lifestages and (2) to examine the impact of exposure scenario and choice of internal dose metric on the adult-child variability factor. For AUCv (Table 6), we observed increased intragroup variability at younger ages following the same trend as Nong et al. (2006) for both bathing and oral exposures with the differences between scenarios being more pronounced for oral exposure (see also Figs. 2A and 3A). For AML all intragroup variability factors approach unity. As discussed in the context of data in Figures 2B and 3B, this is due to metabolism being blood flow limited at environmental exposure levels.

The adult-child variability factor differed substantially between dose metrics and exposure scenarios. Results in Table 6 for parent BDCM exposures (AUCv) differ appreciably between exposure routes. These values demonstrate adult-child factor values for the bathing scenario that range from near-unity (toddler) to a value roughly similar to the assumed default value for toxicokinetic differences among humans (neonate), whereas values for the oral route may exceed five hundred-fold. Differences for the oral route likely reflect the overall higher VmaxC (Supplementary Table 1) and overall metabolic capacity of the adult compared with that of the neonate, combined with a higher internal dose developed following the more temporally concentrated oral exposure scenario as compared with the bathing scenario. Overall trends across age groups were similar to those reported by Nong et al. (2006). Amount metabolized in liver (Table 7) presents a dramatically different picture compared with AUCv. The adult-child factor values for bathing are substantially lower than

1, whereas adult-child factors for the oral exposure approximate unity. Together, these data suggest minimal differences between adults and younger age groups for this dose metric.

The magnitude of differences observed for the adult-child variability factor across exposure scenarios and dose metrics illustrates the importance of identifying the dose metric of greatest concern and considering multiple routes of exposure when appropriate. In the case of a possible role for BDCM in DBP-associated human bladder cancer, available data suggests that extrahepatic metabolism (ie, metabolic activation within urothelial cells) is a key carcinogenic event (Cantor et al., 2010; Ross and Pegram, 2003, 2004). Previous work demonstrated that combined dermal and inhalation exposure results in greater levels of BDCM reaching the systemic circulation compared with ingestion, and thus being available for extrahepatic metabolism (Backer et al., 2000; Kenyon et al., 2016a; Leavens et al., 2007). Taken together, these data highlight the importance of evaluating lifetime, age-specific exposure across multiple routes of exposure to provide the most complete analysis of BDCM internal exposure and hence risk.

When data on the developmental trajectory is available for a variety of XMEs it is also possible to evaluate the impact of transitions in the specific enzymes involved in biotransformation for particular chemicals. For example, Yang et al. (2006) modeled predicted changes in methadone kinetics in pediatric populations 0–24 months of age compared with adults based on measured variability and changes in CYP3A4, CYP3A5, and CYP3A7 expression levels, as well as other physiological parameters using a PBPK model. In addition to the CYP3A family of enzymes (Stevens et al., 2003), similar transitions have been reported for FMO1 transitioning to FMO3 (Koukouritaki et al., 2002). In the case of BDCM, CYP2E1 is the predominant biotransformation enzyme at low substrate concentrations, but both CYP1A2 and CYP3A4 can make substantial contribution to biotransformation at higher substrate concentrations. This raises the question of whether these other enzymes could augment BDCM metabolism if CYP2E1 is not expressed or expressed only at very low levels. Both CYP3A4 and CYP1A2 were measured in the same pediatric livers from which CYP2E1 data used in this study were obtained (McCarver et al., 2017). However, both CYP3A4 and CYP1A2 protein levels were low in the neonate and increased only slowly during the first 6 months to 15 months of life, respectively (Song et al., 2017; Stevens et al., 2003). Thus, in the absence of sufficient CYP2E1 enzyme, substantial CYP3A4 or CYP1A2 contributions to BDCM metabolism would only be predicted in the older age groups and adults.

Our results also demonstrate the potential for higher internal extrahepatic exposure to BDCM in neonates and infants compared with adults (as shown by predicted CVmax and AUCv values), which could be toxicologically significant depending on the chemical. BDCM is carcinogenic in rodents with oral gavage exposure resulting in kidney carcinomas in both rats and mice, as well as large intestine carcinomas in rats (USEPA, 2005). An increased risk for bladder and colon cancer have been reported in epidemiologic studies (Villanueva et al., 2014), with the most compelling evidence being for bladder cancer (Cantor et al., 2010). For environmental contaminants such as BDCM concerns related to metabolism in both target and non-target tissues can be critical (Ross and Pegram, 2004),

and overall there is a paucity of data needed to scale *in vitro* metabolism data to the *in vivo* situation for extrahepatic metabolism, and to characterize the associated variability.

In summary, this work demonstrates that variation observed in XME expression in early life results in greater predicted variability in PK outcomes compared with adults across multiple PK outcomes and routes of exposure. That this variability is observed during simulation of environmentally relevant exposures makes a strong case for its explicit quantitative consideration when performing child-specific risk analyses.

Supplementary Material

Refer to Web version on PubMed Central for supplementary material.

ACKNOWLEDGMENTS

Parts of this work at an earlier stage of development were presented at the 2017 Society of Toxicology Meeting. We thank our colleagues at U.S. EPA/ORD/NCEA and NCCT for their thorough review and helpful suggestions.

Disclaimer:

The research described in this manuscript has been reviewed by the National Health and Environmental Effects Research Laboratory, U. S. Environmental Protection Agency and approved for publication. Approval does not signify that the contents necessarily reflect the views and policies of the agency nor does the mention of trade names or commercial products constitute endorsement or recommendation for use.

REFERENCES

AEgis T. (2010). AcslX Optimum User's Guide. AEgis Technologies, Huntsville, AL.

Backer LC, Ashley DL, Bonin MA, Cardinali FL, Kieszak SM, and Wooten JV (2000). Household exposures to drinking water disinfection by-products: Whole blood trihalomethane levels. J. Exp. Anal. Environ. Epidemiol 10, 321–326.

Barter ZE, Chowdry JE, Harlow JR, Snawder JE, Lipscomb JC, and Rostami-Hodjegan A. (2008). Covariation of human microsomal protein per gram of liver with age: Absence of influence of operator and sample storage may justify inter laboratory data pooling. Drug Metab. Dispos 36, 2405–2409. [PubMed: 18775982]

Batterman S, Zhang L, Wang S, and Franzblau A. (2002). Partition coefficients for the trihalomethanes among blood, urine, water, milk and air. Sci. Total Environ 284, 237–247. [PubMed: 11846168]

Blume-Peytavi U, Tan J, Tennstedt D, Boralevi F, Fabbrocini G, Torrelo A, Soares-Oliveira R, Haftek M, Rossi AB, and Thouvenin MD (2016). Fragility of epidermis in newborns, children and adolescents. J. Eur. Acad. Dermatol. Venereol 30, 3–56.

Brochu P, Brodeur J, and Krishnan K. (2011). Derivation of physiological inhalation rates in children, adults and elderly based on nighttime and daytime respiratory parameters. Inhal. Toxicol 23, 74–94. [PubMed: 21299435]

Brochu P, Brodeur J, and Krishnan K. (2012). Derivation of cardiac output and alveolar ventilation rate based on energy expenditure measurements in healthy males and females. J. Appl. Toxicol 32, 564–580. [PubMed: 21365669]

Brochu P, Ducré-Robitaille JF, and Brodeur J. (2006). Physiological daily inhalation rates for free-living individuals aged 1 month to 96 years, using data from doubly labeled water measurements: A proposal for air quality criteria, standard calculations and health risk assessment. Human Ecol. Risk Assess 12, 675–701.

Brown RP, Delp MD, Lindstedt SL, Rhomberg LR, and Beliles RP (1997). Physiological parameter values for physiologically based pharmacokinetic models. Toxicol. Ind. Health 13, 407–484. [PubMed: 9249929]

Cantor KP, Villanueva CM, Silverman DT, Figueroa JD, Real FX, Garcia-Closas M, Malats N, Chanock S, Yeager M, and Tardon A. (2010). Polymorphisms in GSTT1, GSTZ1, and CYP2E1, disinfection by-products, and risk of bladder cancer in Spain. Environ. Health Perspect 118, 1545–1550. [PubMed: 20675267]

De Bock L, Boussery K, De Bruyne R, Van Winckel M, Stephenne X, Sokal E, and Van Bocxlaer J. (2014). Microsomal protein per gram of liver (MPPGL) in paediatric biliary atresia patients. Biopharm. Drug Dispos 35, 308–312. [PubMed: 24644121]

Edginton AN, Schmitt W, and Willmann S. (2006). Development and evaluation of a generic physiologically based pharmacokinetic model for children. Clin. Pharmacokinet 45, 1013–1034. [PubMed: 16984214]

Gehan EA, and George SL (1970). Estimation of human body surface area from height and weight. Cancer Chemotherapy Reports Pt 1 54, 225–235.

Haddad S, Restieri C, and Krishnan K. (2001). Characterization of age-related changes in body weight and organ weights from birth to adolescence in humans. J. Toxicol. Environ. Health A 64, 453–464. [PubMed: 11732696]

Haddad S., Tardif GC., and Tardif R. (2006). Development of physiologically based toxicokinetic models for improving the human indoor exposure assessment to water contaminants: Trichloroethylene and trihalomethanes. J. Toxicol. Environ. Health A 69, 2095–2136.

Hines RN (2008). The ontogeny of drug metabolism enzymes and implications for adverse drug events. Pharmacol. Ther 118, 250–267. [PubMed: 18406467]

Hines RN (2012). Age-dependent expression of human drug-metabolizing enzymes. In Encyclopedia of Drug Metabolism and Interactions (Lyubimov AV, Ed.), Chpt. 15. John Wiley & Sons, New York.

International Commission on Radiological Protection (ICRP). (2002). Basic anatomical and physiological data for use in radiological protection: reference values. ICRP 89, ed., Valentin J, Pergamon Press, Oxford, United Kingdom.

International Programme on Chemical Safety (IPCS). (2005). Chemical-Specific Adjustment Factors for Interspecies Differences and Human Variability: Guidance Document for Use of Data in Dose/Concentration-Response Assessment. World Health Organization, Geneva.

Johnsrud EK, Koukouritaki SB, Divakaran K, Brunengraber LL, Hines RN, and McCarver DG (2003). Human hepatic CYP2E1 expression during development. J. Pharmacol. Exp. Ther 307, 402–407. [PubMed: 14500779]

Kedderis GL (1997). Extrapolation of in vitro enzyme induction data to humans in vivo. Chem. Biol. Interact 107, 109–121. [PubMed: 9402953]

Kenyon EM, Eklund C, Leavens TL, and Pegram RA (2016a). Development and application of a human PBPK model for bromodichloromethane (BDCM) to investigate impacts of multi-route exposure. J. Appl. Toxicol 36, 1095–1111. [PubMed: 26649444]

Kenyon EM, Eklund C, Lipscomb JC, and Pegram RA (2016b). The impact of variation in scaling factors on the estimation of internal dose metrics: A case study using bromodichloromethane (BDCM). Toxicol. Mech. Methods 26, 620–626. [PubMed: 27595344]

Koukouritaki SB, Simpson P, Yeung CK, Rettie AE, and Hines RN (2002). Human hepatic flavin-containing monooxygenase 1 (FMO1) and 3 (FMO3) developmental expression. Pediatr. Res 51, 236–243. [PubMed: 11809920]

Laurent A, Mistretta F, Bottigioli D, Dahel K, Goujon C, Nicolas JF, Hennino A, and Laurent PE (2007). Echographic measurement of skin thickness in adults by high frequency ultrasound to assess the appropriate microneedle length for intradermal delivery of vaccines. Vaccine 25, 6423–6430. [PubMed: 17640778]

Leavens TL, Blount BC, DeMarini DM, Madden MC, Valentine JL, Case MW, Silva LK, Warren SH, Hanley NM, and Pegram RA (2007). Disposition of bromodichloromethane in humans following oral and dermal exposure. Toxicol. Sci 99, 432–445. [PubMed: 17656487]

Lehman-McKeeman LD (2013). Absorption, distribution and excretion of toxicants, In Casarett and Doull's Toxicology, 8th ed. (Klaassen CD, Ed.), pp.153–184. McGra-Hill, New York.

Lilly PD, Andersen ME, Ross TM, and Pegram RA (1997). Physiologically-based estimation of in vivo rates of bromodichloromethane metabolism. Toxicology 124, 141–152. [PubMed: 9458004]

Lipscomb JC, Garrett CM, and Snawder JE (1997). Cytochrome P450-dependent metabolism of trichloroethylene: Interindividual differences in humans. Toxicol. Appl. Pharmacol 142, 311–318. [PubMed: 9070354]

Lipscomb JC, and Poet TS (2008). In vitro measurements of metabolism for application in pharmacokinetic modeling. Pharmacol. Ther 118, 82–103. [PubMed: 18374419]

Lipscomb JC, Teuschler LK, Swartout J, Popken D, Cox T, and Kedderis GL (2003). The impact of cytochrome P450 2E1-dependent metabolic variance on a risk-relevant pharmacokinetic outcome in humans. Risk Anal. 23, 1221–1238. [PubMed: 14641897]

Lipscomb JC, Teuschler LK, Swartout J, Striley CAF, and Snawder JE (2003). Variance of microsomal protein and cytochrome P450 2E1 and 3A forms in adult human liver. Toxicol. Mech. Methods 13, 45–51. [PubMed: 20021182]

Lynberg M, Nuckols JR, Langlois P, Ashley D, Singer P, Mendola P, Wilkes C, Krapfl H, Miles E, Speight V, et al. (2001). Assessing exposure to disinfection by-products in women of reproductive age living in Corpus Christi, Texas, and Cobb County, Georgia: Descriptive results and methods. Environ. Health Perspect 109, 597–604. [PubMed: 11445514]

Mahle DA, Gearhart JM, Grigsby CC, Mattie DR, Barton HA, Lipscomb JC, and Cook RS (2007). Age-dependent partition coefficients for a mixture of volatile organic solvents in Sprague-Dawley rats and humans. J. Toxicol. Environ. Health A 70, 1745–1751. [PubMed: 17885931]

McCarver DG, Simpson PM, Kocarek TA, James MO, Runge-Morris M, Stevens JC, Yoon M, and Hines RN (2017). Data from: Developmental expression of drug metabolizing enzymes: Impact on disposition in neonates and young children, doi: 10.5061/dryad.71pp6, last accessed October 3, 2018.

McNally K, Cotton R, and Loizou GD (2011). A workflow for global sensitivity analysis of PBPK models. Front. Pharmacol 2, 1–22. [PubMed: 21779246]

Morris MD (1991). Factorial sampling plans for preliminary computational experiments. Technometrics 33, 161–174.

Nong A, McCarver DG, Hines RN, and Krishnan K. (2006). Modeling interchild differences in pharmacokinetics on the basis of subject-specific data on physiology and hepatic CYP2E1 levels: A case study with toluene. Toxicol. Appl. Pharmacol 214, 78–87. [PubMed: 16464483]

Nuckols JR, Ashley DL, Lyu C, Gordon SM, Hinckley AF, and Singer P. (2005). Influence of tap water quality and household water use activities on indoor air and internal dose levels of trihalomethanes. Environ. Health Perspect 113, 863–870. [PubMed: 16002374]

Ploin D, Schwarzenbach F, Dubray C, Nicolas JF, Goujon C, Trong MD, and Laurent PE (2011). Echographic measurement of skin thickness in sites suitable for intradermal vaccine injection in infants and children. Vaccine 29, 8438–8442. [PubMed: 21821081]

Prasad B, Gaedigk A, Vrana M, Gaedigk R, Leeder JS, Salphati L, Chu X, Xiao G, Hop C, Evers R, et al. (2016). Ontogeny of hepatic drug transporters as quantified by LC-MS/MS proteomics. Clin. Pharmacol. Ther 100, 362–370. [PubMed: 27301780]

Price K, Haddad S, and Krishnan K. (2003). Physiological modeling of age-specific changes in the pharmacokinetics of organic chemicals in children. J. Toxicol. Environ. Health A 66, 417–433. [PubMed: 12712630]

Ross MK, and Pegram RA (2003). Glutathione transferase theta 1–1-dependent metabolism of the water disinfection byproduct bromodichloromethane. Chem. Res. Toxicol 16, 216–226. [PubMed: 12588193]

Ross MK, and Pegram RA (2004). In vitro biotransformation and genotoxicity of the drinking water disinfection byproduct bromodichloromethane, DNA binding mediated by glutathione transferase theta 1–1. Toxicol. Appl. Pharmacol 195, 166–181. [PubMed: 14998683]

Saitoh A., Aizawa Y., Sato I., Hirano H., Sakai T., and Mori M. (2015). Skin thickness in young infants and adolescents: Applications for intradermal vaccination. Vaccine 33, 3384–3391. [PubMed: 25944297]

SAS Institute Inc. (2013). SAS/ETSVR 13.1 User's Guide. SAS Institute Inc, Cary, NC.

Sethi PK, White CA, Cummings BS, Hines RN, Muralidhara S, and Bruckner JV (2016). Ontogeny of plasma proteins, albumin and binding of diazepam, cyclosporine, and deltamethrin. Pediatr. Res 79, 409–415. [PubMed: 26571224]

Song G, Sun X, Hines RN, McCarver DG, Lake BG, Osimitz TG, Creek MR, Clewell HJ, and Yoon M. (2017). Determination of human hepatic CYP2C8 and CYP1A2 age-dependent expression to support human health risk assessment for early ages. Drug Metab. Dispos 45, 468–475. [PubMed: 28228413]

Stevens JC, Hines RN, Gu C, Koukouritaki SB, Manro JR, Tandler PJ, and Zaya MJ (2003). Developmental expression of the major human hepatic CYP3A enzymes. J. Pharmacol. Exp. Ther 307, 573–582. [PubMed: 12975492]

Tan YM, Liao KH, and Clewell HJ (2007). Reverse dosimetry: Interpreting trihalomethanes biomonitoring data using physiologically based pharmacokinetic modeling. J. Exp. Sci. Environ. Epidemiol 17, 591–603.

Thomas RS, Lytle WE, Keefe TJ, Constan AA, and Yang RS (1996). Incorporating Monte Carlo simulation into physiologically based pharmacokinetic models using advance continuous simulation language (ACSL): A computational method. Fundam. Appl. Toxicol 31, 19–28. [PubMed: 8998950]

Thomson MMS, Hines RN, Schuetz EG, and Meibohm B. (2016). Expression patterns of OATP1B1 and OATP1B3 protein in human pediatric liver. Drug Metab. Dispos 44, 999–1004. [PubMed: 27098745]

USEPA. (1997). Guiding Principles for Monte Carlo Analysis. Risk Assessment Forum, Washington, DC.

USEPA. (2005). Drinking Water Criteria Document for Brominated Trihalomethanes. Office of Water, Washington, DC. EPA-822-R05–011

USEPA. (2008). Child-Specific Exposure Factors Handbook. Office of Research and Development, National Center for Environmental Assessment, Washington, DC. EPA/600/R-06/096F

USEPA. (2011a). Exposure Factors Handbook. Office of Research and Development, National Center for Environmental Assessment, Washington, DC. EPA/600/R-090/052F

USEPA. (2011b). Toxicological Review of Dichloromethane (Methylene Chloride). EPA/635/R-10/003F. Available at: www.epa.gov/iris, last accessed October 3, 2018.

USEPA. (2014). Guidance for Applying Quantitative Data to Develop Data-Derived Extrapolation Factors for Interspecies and Intraspecies Extrapolation. Office of the Science Advisor, Risk Assessment Forum, Washington, DC, EPA/100/R-14/002F

White DR, Widdowson EM, Woodard HQ, and Dickerson JWT (1991). The composition of body tissues (II) fetus to young adult. Br. J. Radiol 64, 149–159. [PubMed: 2004206]

Villanueva CM, Kogevinas M, Cordier S, Templeton MR, Vermeulen R, Nuckols JR, Nieuwenhuijsen MJ, and Levallois P. (2014). Assessing exposure and health consequences of chemicals in drinking water: current state of knowledge and research needs. Environ. Health Perspect 122, 213–221. [PubMed: 24380896]

Xu X, Mariano TM, Laskin JD, and Weisel CP (2002). Percutaneous absorption of trihalomethanes, haloacetic acids, and haloketones. Toxicol. Appl. Pharmacol 184, 19–26. [PubMed: 12392965]

Yang F, Tong X, McCarver DG, Hines RN, and Beard DA (2006). Population-based analysis of methadone distribution and metabolism using an age-dependent physiologically based pharmacokinetic model. J. Pharmacokinet. Pharmacodynam 33, 485–518.

Yoon M, and Clewell HJ (2016). Addressing early life sensitivity using physiologically based pharmacokinetic modeling and in vitro to in vivo extrapolation. Toxicol. Res 32, 15–20. [PubMed: 26977255]

Young JF., Luecke JH., Pearce BA., Lee T., Ahn H., Baek S., Moon H., Dye DW., Davis TM., and Taylor SJ. (2009). Human organ/tissue growth algorithms that include obese individuals and black/white population organ weight similarities from autopsy data. J. Toxicol. Environ. Health A 72, 527–540. [PubMed: 19267313]

Zhao G, and Allis JW (2002). Kinetics of bromodichloromethane metabolism by cytochrome P450 isoenzymes in human liver microsomes. Chem. Biol. Interact 140, 155–168. [PubMed: 12076522]

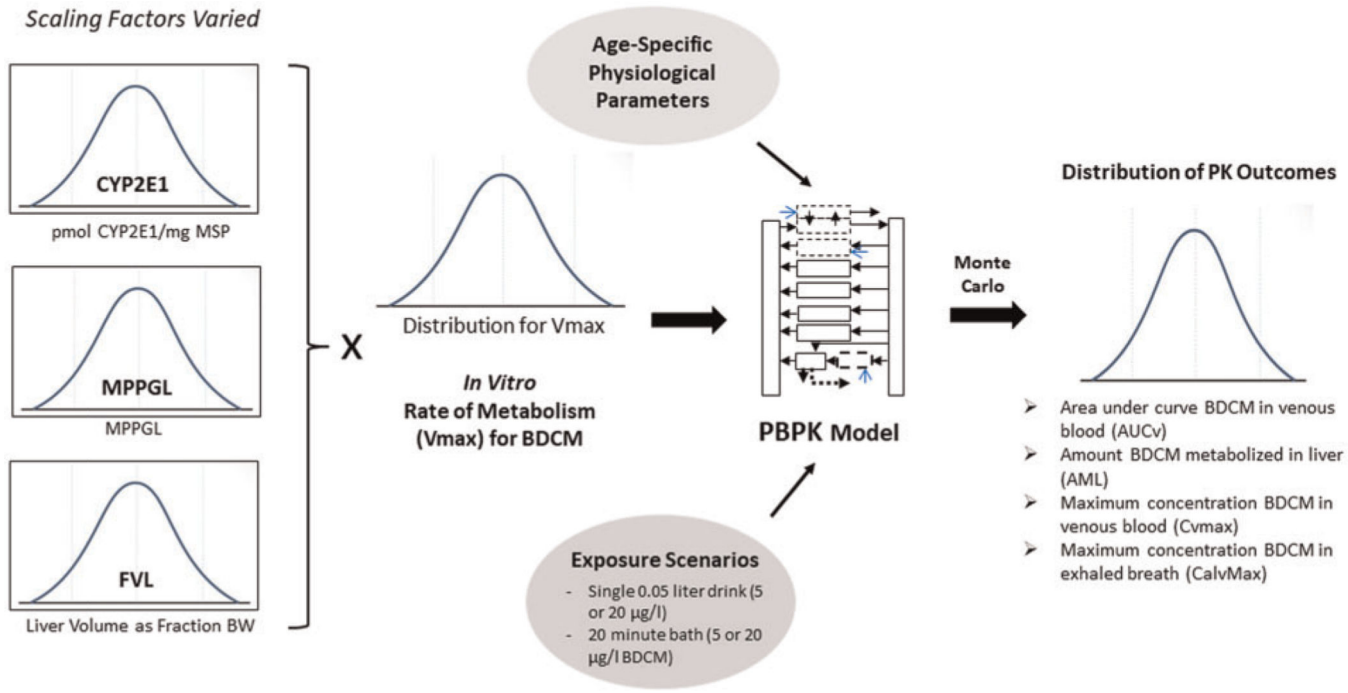

Figure 1.

Diagram illustrating workflow and methodology. The model and subsequent analyses were implemented in acslXtreme 3.0.2.1 (The AEgis Technologies Group; Huntsville, AL).

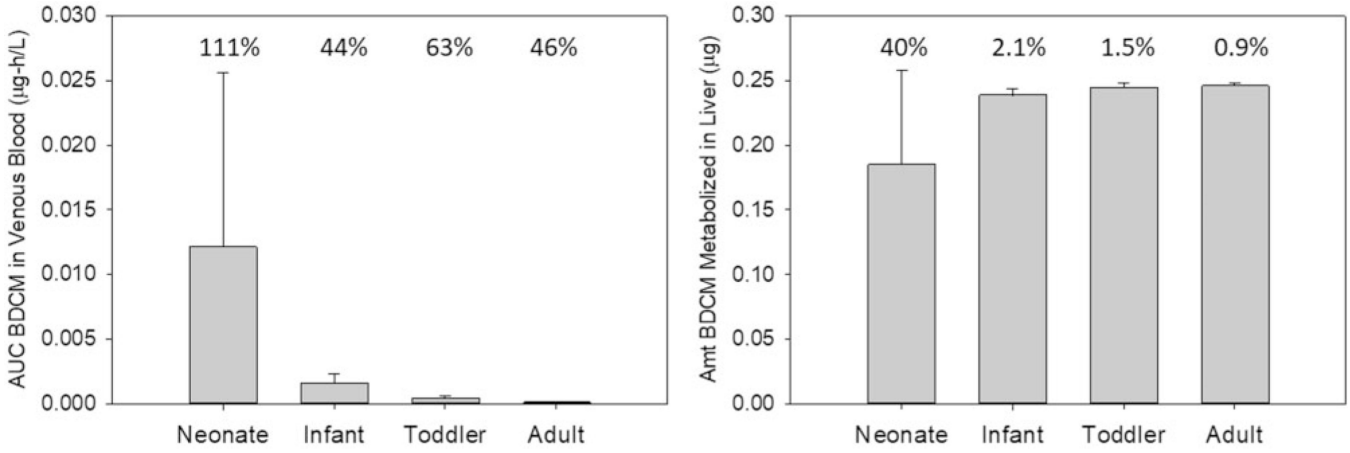

Figure 2.

Comparison of AUC for (A) venous blood BDCM (µg-h/l, $\bar{x} \pm SD$) and (B) amount of BDCM metabolized in liver (µg, $\bar{x} \pm SD$) across age groups based on Monte Carlo simulations (2 h) utilizing the distributional characteristics for FVL, CYP2E1, and MPPGL shown in Table 3 for an oral exposure to water containing 5 µg/l BDCM as a single 0.05-liter drink. The number associated with each bar is the coefficient of variation (%).

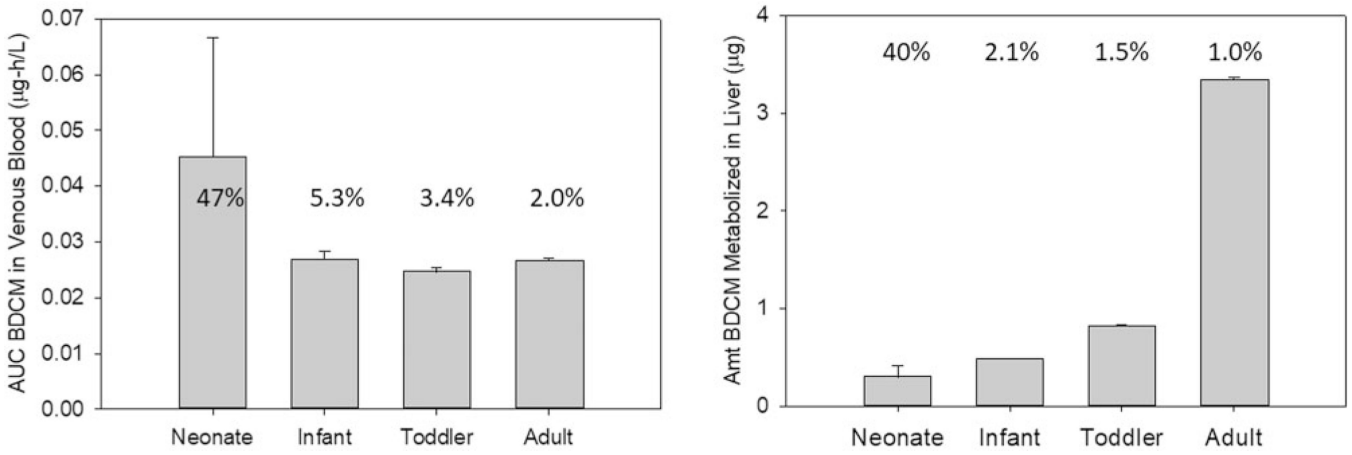

Figure 3.

Comparison of AUC for (A) venous blood BDCM (µg-h/l, $\bar{x} \pm SD$) and (B) amount BDCM metabolized in liver (µg, $\bar{x} \pm SD$) across age groups based on Monte Carlo simulations (2 h) utilizing the distributional characteristics for FVL, CYP2E1 and MPPGL shown in Table 3 for a 20-min bath in water containing 5 µg/l BDCM. The number associated with each bar is the coefficient of variation (%).

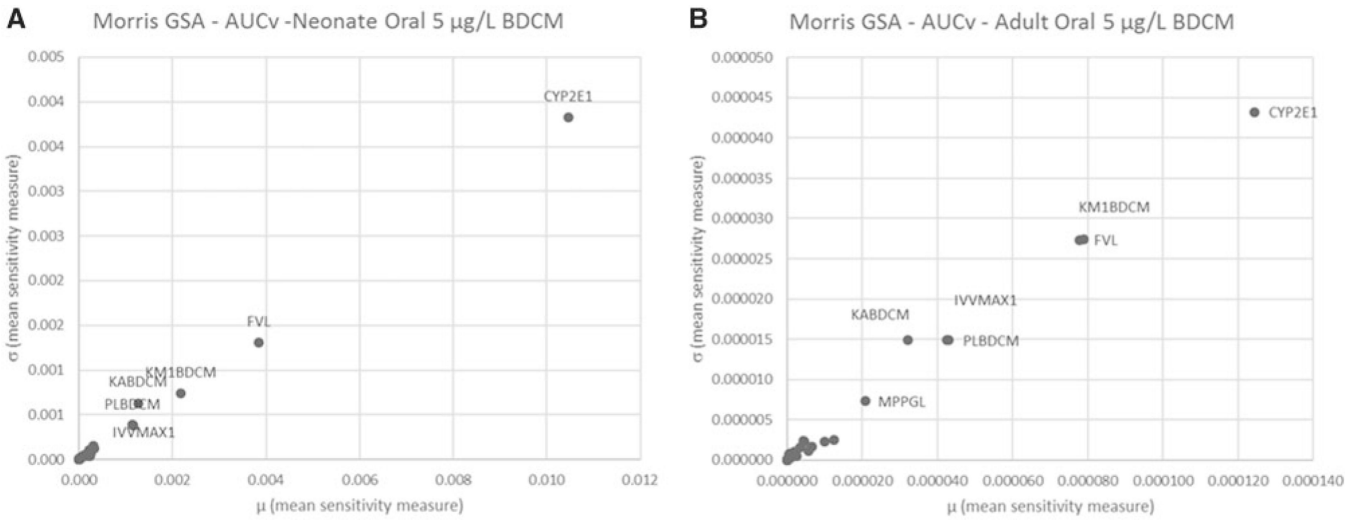

Figure 4.

Morris screening level global sensitivity analysis for oral exposure scenario of a single 0.05 L ingestion of water containing 5 µg/l BDCM for AUCv in (A) neonate and (B) adult. Parameter abbreviations are defined in Tables 1 and 2. Due to space constraints, only the most influential parameters were annotated.

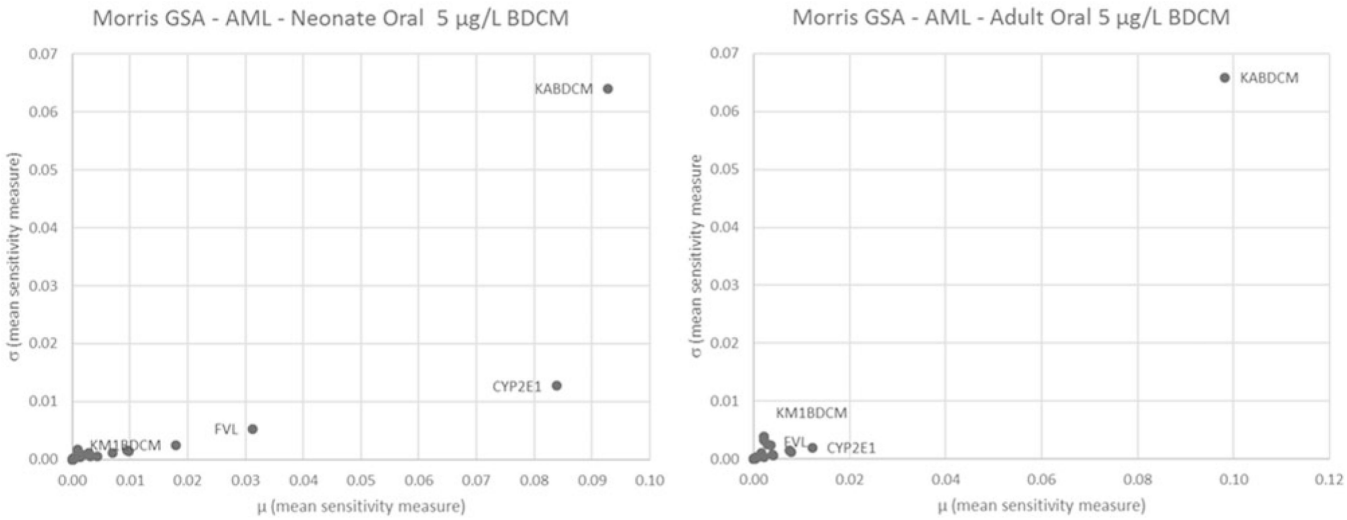

Figure 5.

Morris screening level global sensitivity analysis for oral exposure scenario of a single 0.05 L ingestion of water containing 5 µg/l BDCM for AML in (A) neonate and (B) adult. Parameter abbreviations are defined in Tables 1 and 2. Due to space constraints, only the most influential parameters were annotated.

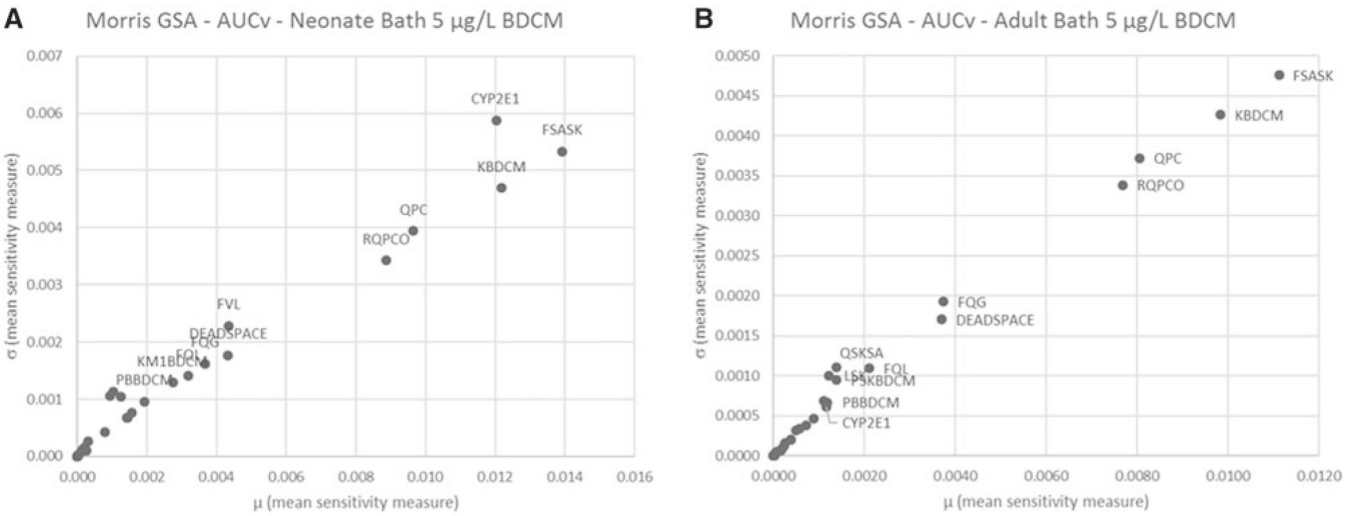

Figure 6.

Morris screening level global sensitivity analysis for bathing exposure for 20 min in water containing 5 µg/l BDCM for AUCv in (A) neonate and (B) adult. Parameter abbreviations are defined in Tables 1 and 2. Due to space constraints, only the most influential parameters were annotated.

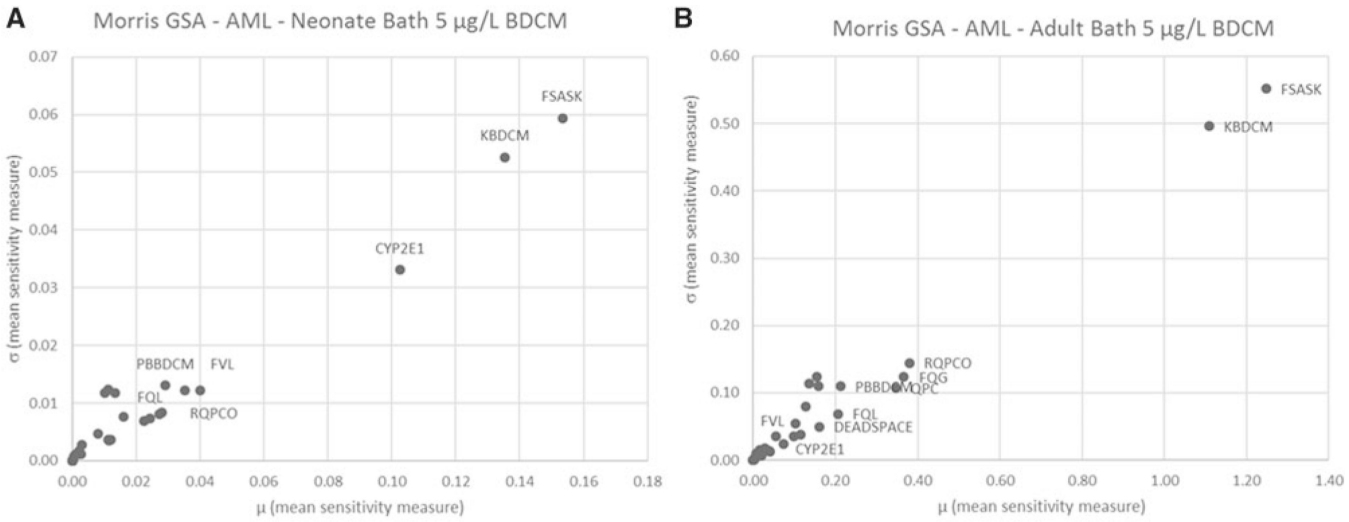

Figure 7.

Morris screening level global sensitivity analysis for bathing exposure for 20 min in water containing 5 µg/l BDCM for AML in (A) neonate and (B) adult. Parameter abbreviations are defined in Tables 1 and 2. Due to space constraints, only the most influential parameters were annotated.

Table 1.

Pediatric and Adult Physiological Parameters for the Human BDCM Model

Parameter, Units	Symbol	Child 0–30 Days	Child 31–90 Days	Child Approx. 1–2 Years	Adult	Note
Height, cm	height	51.8	57.4	81.0	174.7	*1*
Body weight, kg	BW	3.81	5.22	10.55	80.8	*2*
Alveolar ventilation rate, l/h-m^2	QPC	391	432	470	419	*3*
Alveolar deadspace, unitless	deadspace	0.336	0.336	0.336	0.344	*3*
QPC to cardiac output (CO) ratio, unitless	RQPCO	1.0	1.0	1.0	1.0	*4*
Fractional blood flows, unitless						
Richly perfused tissue group	FQRP	0.75	0.75	0.75	0.75	*5, 7*
Liver	FQL	0.13	0.13	0.13	0.09	*5, 6*
Gastrointestinal tract	FQG	0.15	0.15	0.12	0.16	*5, 6*
Kidney	FQK	0.13	0.13	0.14	0.15	*5, 6*
Poorly perfused tissue group	FQPP	0.25	0.25	0.25	0.25	*5, 7*
Fat	FQF	0.04	0.04	0.05	0.05	*5, 6*
Blood flow to skin, l/min-m^2	QSKSA	0.58	0.58	0.58	0.58	*5, 7*
Compartment volume, unitless						
Blood fraction of BW	FVBD	0.0671	0.0617	0.0529	0.079	*5, 8*
Blood as arterial	FVART	0.25	0.25	0.25	0.25	*5*
Blood as venous	FVVEN	0.75	0.75	0.75	0.75	*5*
Richly perfused fraction of BW	FVRP	0.2	0.2	0.2	0.2	*5*
Poorly perfused fraction of BW	FVPP	0.8	0.8	0.8	0.8	*5*
GI tract fraction of BW	FVGI	0.0146	0.0146	0.0177	0.0165	*5, 8*
Liver fraction of BW	FVL	0.0355	0.0355	0.0382	0.026	*5, 8*
Fat fraction of BW	FVF	0.169	0.174	0.175	0.21	*8*
Kidney fraction of BW	FVK	0.0065	0.0065	0.0066	0.004	*5, 8*
Volume GI tract lumen, L	VLUM	0.14	0.14	0.24	2.1	*5, 9*
Skin thickness, mm	LSK	1.3	1.3	1.3	2.0	*5, 10*

*1*Calculated based on midpoint of age range for 50th percentile from CDC data tables for length-for-age for male and female children. https://www.cdc.gov/growthcharts/who_charts.htm#The WHO Growth Charts, last accessed October 3, 2018. For adult, used mean combined male and female, aged 30–40 years (Table 8–3, USEPA, 2011a).

[2]Calculated based on midpoint of age range for 50th percentile from CDC data tables for weight-for-age for male and female children. https://www.cdc.gov/growthcharts/who_charts.htm#The WHO Growth Charts, last accessed October 3, 2018. For adult used combined male and female, aged 30–40 mean (Table 8–16, USEPA, 2011a).

[3]Derived from mean of alveolar ventilation rate male and female children at approx. 1 month in Brochu et al. (2006), and 0.22–0.5 years for 30–90 dys group, 1–2 years of age and adults (35–40 years) in Brochu et al. (2011). Deadspace figures from Brochu et al. (2012) with childhood age groups assumed same and set to mean value for youngest age group (5–10 years) and 35- to 45-year age group for adults. Minute ventilation rate is scaled to skin surface area (SA) in m^2 in the model; $QP = QPC^{*}SA^{*}$ (1-Deadspace). $SA = Height^{(0.725)} * Weight^{(0.425)} * 0.007187$ in m^2 from (Adams, 1993; also eq. 6–3 in USEPA, 2008) for all childhood age groups. For adults use equation, $SA = Height^{(0.417)} * Weight^{(0.517)} * 0.02350$ in m^2 (Gehan and George, 1970, also eq. 7A-3 USEPA, 2011a).

[4]Cardiac Output, $QC = QP/RQPCO$.

[5]Adult value same as in original model.

[6]Blood flows calculated from Edginton et al. (2006) for 0–30 (newborn) and 1 year-old, 31–90 days assumed same as newborn. Fractional blood flows to individual tissues are scaled to cardiac output (QC), ie, $QL = FQL^{*}QC$, $QG = FQG^{*}QC$, $QK = FQK^{*}QC$, and $QF = FQF^{*}QC$.

[7]Richly (QRP) and poorly perfused (QPP) tissues calculated by difference subtracting out blood flows from liver, kidney, and gut for QRP and subtracting out fat and skin volumes for QPP, ie, $QRP = \left(FQRP^{*}QC\right) - QL - QK - QG$ and $QPP = \left(FQPP^{*}QC\right) - QF - QSK$. Blood flow to skin (QSK) is scaled on the basis of body surface area, ie, $QSK = QSKSA^{*}SA^{*}60\ min/h$. Total liver blood flow is sum of liver plus gut as shown in Supplementary Figure 1.

[8]Calculated as fraction of BW using estimated mass based on equations from Haddad et al. (2001) using average of male and female and midpoint of age range. FVL is included for completeness; Monte Carlo analysis uses FVL distributional descriptors specific for each age group in Table 3. Blood volume assumes density of 1 g/l. Fat volume is recalculated from equations of Haddad et al. (2001) based on modifications in Price et al. (2003). Volume of blood compartment is scaled to BW and volume of arterial and venous compartments are scaled to total blood volume. Tissue volumes to tissues are scaled to BW with richly (VRP) and poorly perfused (VPP) tissue volumes calculated respectively, as follows: $VRP = FVRP^{*}BW - VL - VGI - VBD - VK$ and $VPP = FVPP^{*}BW - VL - VSK$. Volume of skin (VSK) is calculated as $VSK = LSK^{*}SA$.

[9]Estimated based on figures in ICRP (2002, Table 2.8, p. 18) for newborn and 1-year old; age range of 31–90 days assumed to be same as 0–30 days.

[10]LSK is average value for thickness of dermis and epidermis for adults (Laurent et al., 2007) and all pediatric age groups (Ploin et al., 2011). Note that skin thickness remains relatively unchanged based on age (up to 5 years), BMI, gender, and skin phototype (Ploin et al., 2011).

Table 2.

Chemical-Specific Parameters in the Human BDCM Model

Parameter, Units	Symbol	Value	Note
Partition coefficients, unitless			
Blood:air	PBBDCM	15.97	*1*
Liver:blood	PLBDCM	1.93	*1*
Gut:blood	PGBDCM	1.93	*2*
Kidney:blood	PKBDCM	2.08	*1*
Fat:blood	PFBDCM	33.2	*1*
Skin:blood	PSKBDCM	2.91	*3*
RPTG:blood	PRPBDCM	1.93	*2*
PPTG:blood	PPPBDCM	0.78	*1*
Skin diffusion coefficient, cm/h	KBDCM	0.18	*4*
Skin:water partition coefficient	PWSBDCM	5.6	*4*
Oral absorption coefficient, h^{-1}	KABDCM	8.3	*5*
Vmax CYP Liver, μg/h-pmol CYP2E1	IVVMAX	0.201	*6*
KM CYP Liver, μg/l	KM1BDCM	221	*6*
Kf GST Liver, 1/h-kg $BW^{0.75}$	VFCBDCM	0.0079	*7*

1 Calculated by dividing rat tissue:air partition coefficient (Lilly et al., 1997) by human blood:air partition coefficient from Kenyon et al. (2016a,b).

2 Gut:air and rapidly perfused tissue:air partition coefficients were assumed to be the same as liver:air.

3 Skin:air partition coefficient (Haddad et al., 2006) used with human blood air partition coefficient to calculate skin:blood partition coefficient.

4 Skin diffusion coefficient determined with method using aqueous solution across human skin (Xu et al., 2002). Skin:water partition coefficient calculated on basis of water:air partition coefficient (Batterman et al., 2002) divided by skin:air partition coefficient (Haddad et al., 2006).

5 Estimated on basis of Tmax from oral time course data of Leavens et al. (2007) and assumed to be the same across age groups.

6 Experimentally determined in pooled adult human microsomes as 1.74 nmoles/min–mg MSP (Kenyon et al., 2016a) and converted to 17.14 mg/h-mg MSP in (Kenyon et al., 2016b) analysis. Converted to basis of CYP 2E1 for this analysis using known average CYP2E1 content (85 pmol CYP2E1/mg MSP) for independent set of adult samples for which both CYP2E1 content and P450 content are known at the level of the individual subject Lipscomb (personal communication).

7 Estimated from *in vitro* clearance of BDCM from pooled human liver cytosol (Ross and Pegram 2003).

Table 3.

Parameter Distributions and Values Used As Input to Monte Carlo Analysis for Pediatric Age Groups and Adults

Parameters[a]	**FVL**		**MPPGL**		**CYP2E1**	
Age Group	**Distribution and Descriptors**[b]	**Value**	**Distribution and Descriptors**	**Value**	**Distribution and Descriptors**	**Value**
0–30 days, neonate	Normal		Log normal		Gamma	
	Mean	0.0412	GM	25.55	Alpha	0.505
	SD	0.0157	GSD	1.001	Theta	26.6
	Lower limit	0.0114	Lower limit	25.53		
	Upper limit	0.0775	Upper limit	25.60		
31–90 days, infant	Normal		Log Normal		Gamma	
	Mean	0.0366	GM	25.68	Alpha	10.7
	SD	0.0102	GSD	1.002	Theta	2.24
	Lower limit	0.0145	Lower limit	25.61		
	Upper limit	0.0612	Upper limit	25.74		
91 days–2 years, toddler	Normal		Log Normal		Gamma	
	Mean	0.0445	GM	26.35	Alpha	4.82
	SD	0.0159	GSD	1.028	Theta	9.42
	Lower limit	0.0274	Lower limit	25.76		
	Upper limit	0.1200	Upper limit	27.36		
Adult	Normal		Log Normal		Gamma	
	Mean	0.0239	GM	35.24	Alpha	11.1
	SD	0.0090	GSD	1.094	Theta	5.33
	Lower limit	0.0136	Lower limit	29.26		
	Upper limit	0.0415	Upper limit	40.19		

[a]FVL (g liver/kg BW, assuming a volumetric density of 1) and CYP2E1 (pmol/mg microsomal protein) were calculated from data in Johnsrud et al. (2003) for specific pediatric age groups. FVL for adults was recalculated from Young et al. (2009). CYP2E1 for adults is from Lipscomb et al. (1997, 2003a, b). MPPGL was estimated on the basis of the equation published in Barter et al. (2008) using subject age in years for all age groups.

[b]Lower and upper limits are lowest and highest values from data, respectively. Abbreviations: SD, standard deviation; GM, geometric mean; GSD, geometric standard deviation. GM and GSD are log transformed for input into acslx MC routines. For the gamma distribution, alpha is the shape parameter and theta is the scale parameter.

Table 4.

Statistical Characteristics for Maximum Concentration of BDCM in Blood (CVmax) Based on Monte Carlo Analysis Following Oral Exposure (Single 0.05 L Drink, 5 μg/l BDCM in Water, 2 h Simulation)

Age Group	Mean ± SD (ng/l)	% CV	5th Percentile	95th Percentile	Ratio[a]
Neonate	24.1 ± 19.1	79.2	2.57	58.6	22.8
Infant	5.39 ± 2.09	38.7	2.83	9.28	3.28
Toddler	1.32 ± 0.77	57.9	0.52	2.75	5.28
Adult	0.23 ± 0.10	43.4	0.11	0.41	3.75

[a]Ratio of 95th to 5th percentile values.

Table 5.

Statistical Characteristics for Maximum Concentration of BDCM in Blood (CVmax) Based on Monte Carlo Analysis Following Bathing Exposure (20 min, 5 μg/l BDCM in Water, 2 h Simulation)

Age Group	Mean ± SD (ng/l)	% CV	5th Percentile	95th Percentile	Ratio[a]
neonate	86.8 ± 23.0	26.5	63.53	132.3	2.08
infant	61.8 ± 2.35	3.80	59.06	66.20	1.12
toddler	56.5 ± 1.39	2.45	55.17	59.08	1.07
adult	49.0 ± 0.49	1.00	48.39	49.87	1.03

[a]Ratio of 95th to 5th percentile values.

Table 6.

Intragroup and Adult-Child Variability Factors Derived From AUC for BDCM in Venous Blood (AUCv) for Pediatric Age Groups and Adults for Bathing and Oral Scenarios (5 μg/l BDCM in Water)

Age Group	Scenario	AUCv (μg-h/l)			Intragroup Factor[a]	Adult-Child Factor[b]
		5th%	50th%	95th		
Neonate	Bath	0.0270	0.0351	0.0940	2.68	3.55
Infant		0.0252	0.0265	0.0294	1.11	1.11
Toddler		0.0238	0.0244	0.0261	1.07	0.99
Adult		0.0260	0.0265	0.0276	1.04	
Neonate	Oral	7.26E-04	5.70E-03	4.31E-02	7.57	558
Infant		8.02E-04	1.46E-03	2.92E-03	2.00	37.8
Toddler		1.52E-04	3.42E-04	8.60E-04	2.52	11.1
Adult		3.95E-05	7.72E-05	1.59E-04	2.06	

[a]The intragroup variability factor was calculated as the ratio of the 95th percentile value over the 50th percentile value for the same age group.

[b]The adult-child variability factor was calculated as the ratio of the 95th percentile value for the child over the 50th percentile value for the adult.

Table 7.

Intragroup and Adult-Child Variability Factors Derived From Amount of BDCM Metabolized in Liver (AML) for Pediatric Age Groups and Adults for Bathing and Oral Scenarios (5 μg/l BDCM in Water)

		AML (μg)				
Age Group	**Scenario**	**5th%**	**50th%**	**95th**	**Intragroup Factor[a]**	**Adult-Child Factor[b]**
Neonate	Bath	0.023	0.358	0.401	1.12	0.12
Infant		0.464	0.486	0.495	1.02	0.15
Toddler		0.799	0.825	0.834	1.01	0.25
Adult		3.275	3.345	3.377	1.01	
Neonate	Oral	0.014	0.220	0.246	1.12	1.00
Infant		0.229	0.240	0.244	1.02	0.99
Toddler		0.238	0.245	0.248	1.01	1.01
Adult		0.241	0.246	0.248	1.01	

[a]The intragroup variability factor was calculated as the ratio of the 95th percentile value over the 50th percentile value for the same age group.

[b]The adult-child variability factor was calculated as the ratio of the 95th percentile value for the child over the 50th percentile value for the adult.